Electronic Supplementary Material (ESI) for RSC Advances

Designing left-handed structures from right-handed building blocks

Scott W. Olesen[1], Szilard N. Fejer[2], Dwaipayan Chakrabarti[1], and David J. Wales[1*]

[1]*Department of Chemistry, University of Cambridge,*

Lensfield Road, Cambridge, UK and

[2]*Department of Chemical Informatics,*

Faculty of Education, University of Szeged,

Boldogasszony sgt. 6, H-6725, Szeged, Hungary[†]

(Dated: May 29, 2013)

*dw34@cam.ac.uk

[†]Also at Provitam Foundation, str. Caisului nr. 16, Cluj-Napoca, Romania

Supplementary Information

I. THE PARAMONOV-YALIRAKI POTENTIAL

We used the Paramonov-Yaliraki (PY) potential to model the interactions between the ellipsoidal sites in different building blocks [1]. Each PY site is represented in terms of two shape matrices, one repulsive and one attractive, which modulate the respective interactions between two such sites. The pairwise energy of PY sites is Lennard-Jones-like: the repulsive contribution depends on the distance of closest approach between the repulsive ellipsoids of the two sites, and the attractive contribution similarly depends on the distance of closest approach between the attractive ellipsoids. The pairwise energy for two sites is

$$4\epsilon_0 \left[\left(\frac{\sigma_0}{d_R^{(\mathrm{rep})} + \sigma_0} \right)^{12} - \left(\frac{\sigma_0}{d_R^{(\mathrm{att})} + \sigma_0} \right)^{6} \right], \tag{1}$$

where ϵ_0 is an energy scale, σ_0 is the interaction range, and d_R is an approximation of the distance of closest approach between the relevant ellipsoids. Specifically, d_R is the minimum contact distance between the two ellipsoids along a vector parallel to the intercenter separation. It can be computed using $d_R = r(1 - F^{-1/2})$, where r is the intercenter distance and F is the orientation- and distance-dependent elliptic contact function between the relevant ellipsoids [2, 3]. When the two ellipsoids overlap, $F < 1$. When they do not overlap, $F > 1$. At $F = 1$, the two ellipsoids are externally tangent. In this study, we employ a system of reduced units by setting $\epsilon_0 = \sigma_0 = 1$.

The individual PY sites are parameterized by the shapes of the repulsive and attractive ellipsoids, which are described by the three repulsive semiaxes, a_{1i}, and the three attractive semiaxes, a_{2i}. The parameterization used in this study is depicted in Fig. 1. The repulsive and attractive ellipsoids are ellipsoids of revolution, and there are two free parameters: the polar semiaxis, a_{13}, which is common to both the repulsive and attractive ellipsoids, and the attractive equatorial semiaxis, a_{21}. Both a_{13} and a_{21} were systematically varied to elucidate design principles for the building blocks described below. A visualization of the potential associated with some of the parameterizations used in this study is shown in Fig. 2.

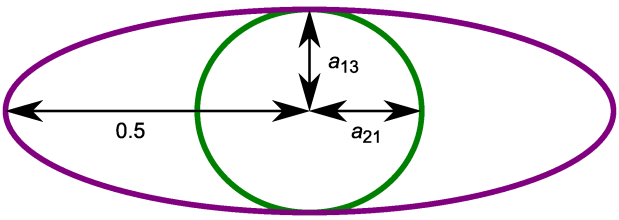

FIG. 1. Cross-section of a Paramonov-Yaliraki site as parameterized in this study, showing the repulsive ellipsoid (purple), the attractive ellipsoid (green), the repulsive equatorial semiaxis (0.5), the attractive equatorial semiaxis, a_{21}, and the polar semiaxis, a_{13}, common to both ellipsoids. In these parameterizations, the two ellipsoids have a common equatorial plane and the same north and south poles.

II. SIMULATION METHODS

Translational perturbations of each building block were uniformly distributed in a sphere with a radius of the same order as the size of the building block (about two reduced units) and the orientational perturbations were uniformly distributed over an interval of approximately one radian. Perturbations that produced overlap were discarded. If three sets of randomly-selected starting coordinates all produced the same lowest minimum, we accepted this structure as the putative global minimum. Otherwise we increased the number of basin-hopping steps until this criterion was met.

In studies of the structures formed by single PY sites, only a few hundred basin-hopping steps were required to reach consistency between runs starting from distinct configurations [4]. However, for the bowtie building blocks, tens of thousands of steps were required to reach the same kind of consistency. The increase in landscape complexity is probably due to the differences in the interaction range parameters, σ_0, used in the two studies. The study of single-site PY building blocks used $\sigma_0 = 1$, 18, and 30, while in this study we used only $\sigma_0 = 1$. Decreasing the interaction length scales probably makes the energy landscape rougher [5–7], which makes it more difficult to locate the global minima.

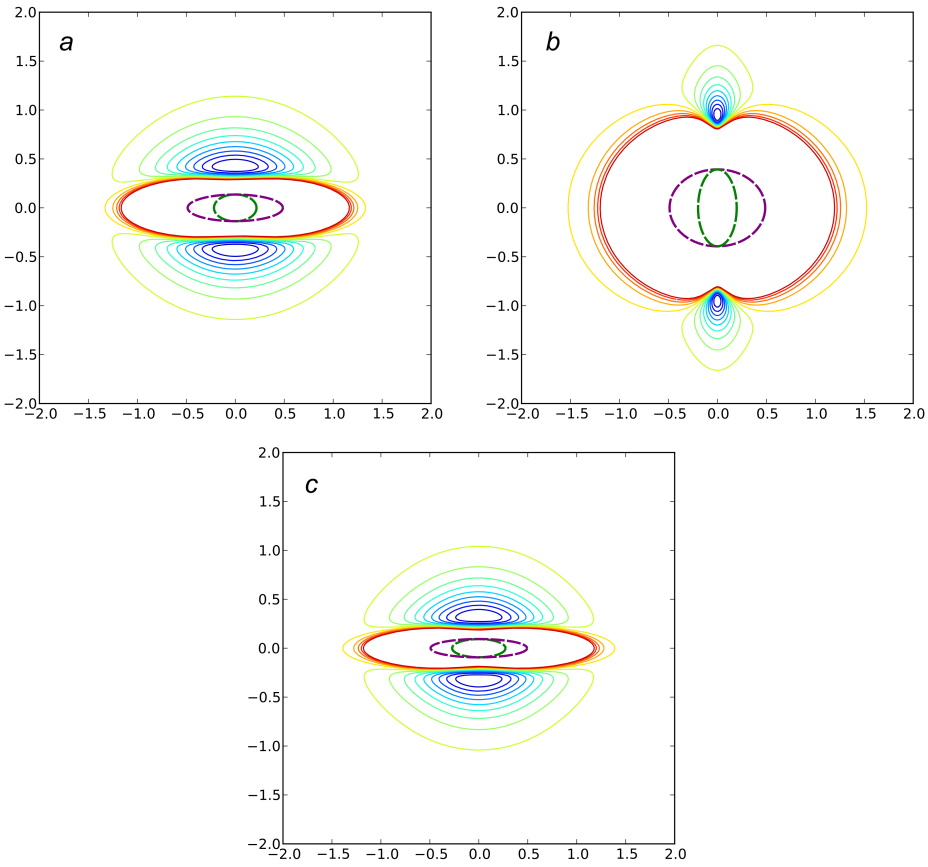

FIG. 2. Lines of equipotential for the PY potential for the featured parameterizations. This figure shows a 2D slice of the potential energy landscape for two PY sites. The orientations of the two sites are fixed as identical so that the potential energy depends only on the relative angle and separation between the two sites. In each subfigure, the dashed drawing at the center shows the ellipsoids that parameterize the sites. High energies are red; low energies are blue. In general, the sites are "sticky" at the north and south poles but repulsive along the equator. *a*) Sites with intermediate anisotropy ($a_{13} = 0.15$, $a_{21} = 0.28$). *b*) Sites with nearly isotropic repulsive ellipsoids ($a_{13} = 0.41$, $a_{21} = 0.1$). *c*) Highly anisotropic sites ($a_{13} = 0.1$, $a_{21} = 0.23$).

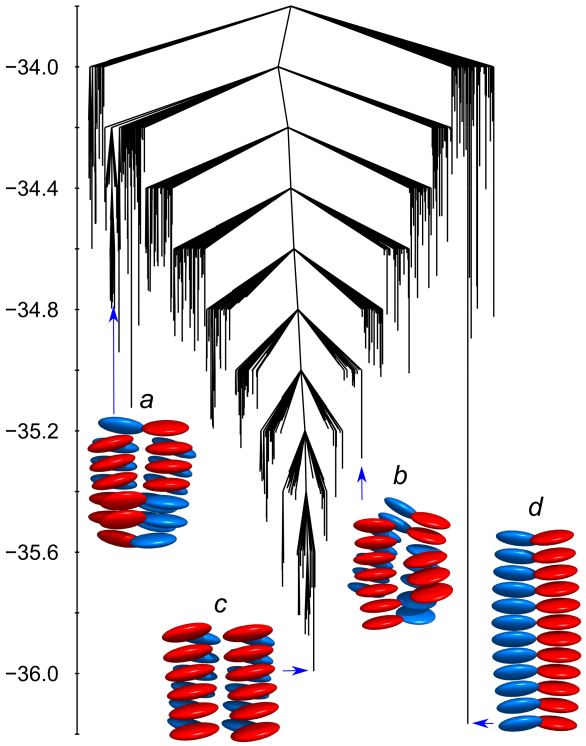

FIG. 3. Part of the disconnectivity graph for 12 bowtie building blocks ($a_{13} = 0.15$, $a_{21} = 0.28$, $\phi = 23°$), showing the organization of the landscape for the minima at the bottom of the main funnel. Energies are measured in ϵ_0. In this example, the main funnel consists of minima that have two helical strands. In some minima, like minimum *a*, the two strands are joined. In others, like minimum *b*, 'caps' sit on top of or below the two strands. The bottom of the main funnel, minimum *c*, has two strands of equal length. The global minimum *d*, which is separated from the rest of the minima by a high barrier, is a single helix for this parameterization.

III. RESULTS

A. A parameterization leading to a frustrated landscape

Not all parameterizations a_{13}, a_{21}, and ϕ produce self-assembling landscapes. An example of a frustrated landscape is shown in Fig. 3.

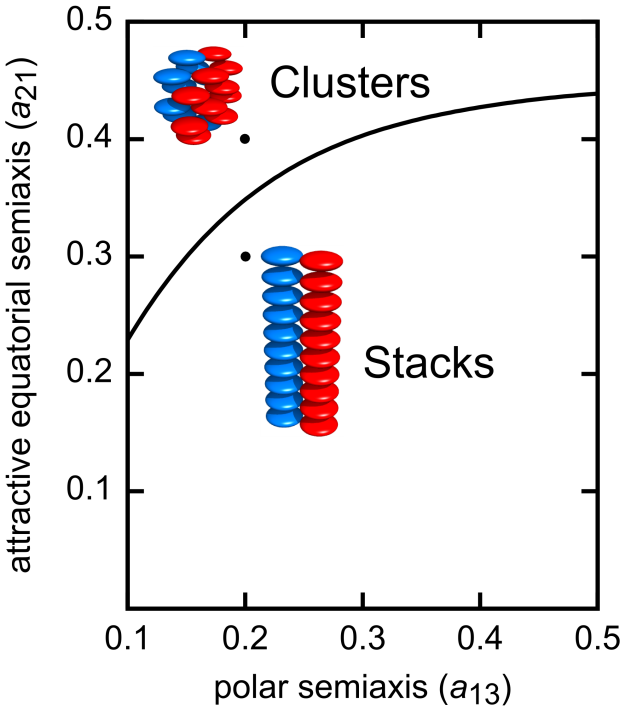

FIG. 4. Regions of the parameter space of a_{13} and a_{21} for which the global minima of clusters composed of bowtie building blocks with $\phi = 0°$ consist of either stacks or more isotropic clusters of bowties. Two global minima for $N = 10$ and two parameterizations (black dots) are shown: one stack ($a_{13} = 0.2$, $a_{21} = 0.3$) and one cluster ($a_{13} = 0.2$, $a_{21} = 0.4$).

B. Regions of the parameter space that produce stacks

Fig. 4 shows the parts of this parameter space in which the global minimum energy configuration consists of stacks when the parameter ϕ is fixed at 0°.

C. Rotation angle depends on building block anisotropy

The rotation angle Ω that minimizes the potential energy of a helix of building blocks depends on the shape parameters a_{13} and a_{21} and on the dihedral angle ϕ. Fig. 5 shows this dependence over most of the parameter space we explored for $\phi = 30°$ and 60°. All relevant strand-like structures assembled from $\phi = 0°$ building blocks have $\Omega = 0°$.

The angles Ω are nearly 90° for parameterizations near $a_{13} = a_{21} = 90°$ (upper-right in Fig. 5). Paramonov-Yaliraki sites with $a_{ij} = 0.5$ for $i, j \in \{1, 2, 3\}$ have anisotropic interactions similar to Lennard-Jones particles. Pairs of Lennard-Jones particles joined

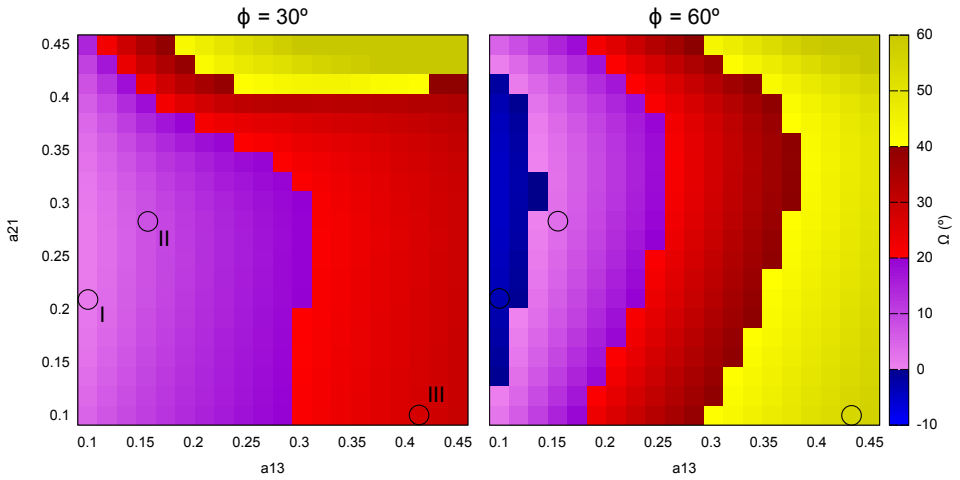

FIG. 5. The rotation angle Ω that minimizes a helix's potential energy is a function of the shape parameters. Each square is colored according to the Ω that minimized the potential energy of a helix with $N = 10$ building blocks with the corresponding a_{13}, a_{21}, and ϕ. Approximate locations of the three building block families I, II, and III are shown with open circles.

in this configuration have stable configuration with building blocks stacked at 90° to one another. The optimal helix configurations for building blocks with a_{13} and a_{21} near 0.5, then, approaches this perpendicularly-stacked configuration, and their optimal Ω values approach 90°.

Left-handed helices (blue in Fig. 5 are optimal only for a small part of the parameter space. This region has very small a_{13}, corresponding to very flat, disc-like sites, and intermediate a_{21}, corresponding to attractive ellipsoids that are neither perfectly rod-like nor extending to the edges of the repulsive ellipsoid. This delicate balance of anisotropies in the repulsive and attractive ellipsoids in each site is necessary for the reversed handedness of the helices.

D. Changes in morphology of the global minimum can be predicted

Because the global minima are generally helical in the region of parameter space we considered, it is useful to define a reduced potential energy landscape $U(\Omega, d)$ whose coordinates are the two parameters that describe a single helix: the distance d between the centers of adjacent bowtie building blocks and the rotation angle Ω. Because d is usually peripheral to the investigation of chirality, the potential energy landscape can be further reduced to

one with a single coordinate Ω by defining

$$\widetilde{U}(\Omega) = \min_d U(\Omega, d). \tag{2}$$

The function $\widetilde{U}$ is well-defined because U has only one minimum in d with Ω fixed.

The $\widetilde{U}$ landscape is useful for identifying morphological transitions in the parameter space. For example, $\widetilde{U}$ for bowties with $\phi = 0°$ and a low value for the attractive equatorial semiaxis a_{21} has one minimum at $\Omega = 0°$. For larger a_{21}, a local minimum of higher energy forms at $\Omega = 90°$. As a_{21} increases, the energy of the $\Omega = 90°$ minimum decreases and the energy of the $\Omega = 0°$ minimum increases, and we expect the local topology to be described by a fold catastrophe [8, 9]. At a critical value of a_{21}, the two minima are equal in energy. At this point in the parameter space, the $\Omega = 0°$ minimum is no longer the global minimum as viewed in the reduced energy landscape with coordinates d and Ω. It is also at precisely this value of a_{21} that the configuration corresponding to the minimum in $\widetilde{U}$ is no longer a local minimum in the complete $6N$-dimensional landscape, where N is the number of building blocks. Hence this value of a_{21} represents the boundary of the helix-forming part of the parameter space for $\phi = 0°$ shown in Fig. 4. A similar analysis applies for $\phi \neq 0°$, but here the minima in $\widetilde{U}$ are displaced away from $\Omega = 0°$ due to the broken symmetry.

In general, increasing a_{21} out of the helix-producing region of the parameter space yields structures that are more and more isotropic. At first, the helix breaks into a 'ladder' where adjacent bowties are staggered. For higher values, the helix bends over and loses its helical topology. For very high values of a_{21}, the potential energy minima are clusters with no particular directionality (Fig. 4).

The energy of the helices increases as ϕ increases until some maximum value of ϕ. This critical value decreases from about 60° for larger a_{21} down to 0° as a_{21} reaches the boundary where the morphology of the global minimum changes for $\phi = 0°$ (Fig. 4). Increasing ϕ beyond this value causes the helix to collapse into a more isotropic cluster. The increased energy and consequently decreasing stability are due to the increasing distance of closest approach between attractive ellipsoids in the same chain.

E. Linear relationship for chiral parameters for $a_{13} \ll a_{21}$

Consider a dimer of building blocks aligned along a single axis like they are in the stacks and helices. The distance between the in-chain attraction between corresponding attractive ellipsoids in the two building blocks is a complicated function of their orientations. As an approximation, consider the distance between the "South Pole" of the attractive ellipsoid in one half of the upper building block and the "North Pole" of the attractive ellipsoid in the corresponding half of the lower building block.

If the distance between the centers of the bowties were fixed at d, the distance between the two poles would be

$$\left\{ \left[a_{21}(1-\cos\Omega) - a_{13}\sin\frac{\phi}{2}\sin\Omega \right]^2 + \left[-a_{21}\sin\Omega + a_{13}\sin\frac{\phi}{2}(1+\cos\Omega) \right]^2 + \left[2a_{13}\cos\frac{\phi}{2} - d \right]^2 \right\}^{1/2}, \quad (3)$$

which is minimized when

$$\Omega^* = \arctan\left[\frac{2\,(a_{13}/a_{21})\sin(\phi/2)}{1-(a_{13}/a_{21})^2\sin^2(\phi/2)} \right]. \quad (4)$$

Comparing to the double-angle formula for the tangent shows that

$$\Omega^* = 2\arctan\left(\frac{a_{13}}{a_{21}}\sin\frac{\phi}{2} \right). \quad (5)$$

For $a_{13} \ll a_{21}$, $\Omega^* \approx 2\,(a_{13}/a_{21})\sin(\phi/2)$. Since $2\sin(\phi/2) \approx \phi$ to within 5% for $0^\circ < \phi < 60^\circ$, we see that $\Omega^* \approx (a_{13}/a_{21})\,\phi$. This analysis quantitatively predicts the slope of the linear parts of the $\Omega(\phi)$ curves.

Decreasing the attractive equatorial semiaxis a_{21} increases the range of ϕ over which Ω is linear. In the limit $a_{21} \to 0$, the attractive ellipsoids reduce to rods whose endpoints lie at the poles of the two ellipsoids. The point of closest approach between the attractive ellipsoids in a chain will be at the ends of rods. In this case, it is clear that in-chain attraction favors minimization of the distance between the poles of the two ellipsoids.

F. Geometrical trends

The spacing between the bowties along the axis of the helix depends nearly linearly on the polar semiaxis a_{13} according to $d \approx 2.3\,a_{13}$ when ϕ is small. The value of the attractive

equatorial semiaxis a_{21} has little effect on d, since the organization of the helix along its axis is due mostly to the polar axes rather than the equatorial axes. Values of d differ significantly from the small ϕ limit when cross-chain repulsion begins to influence Ω, since then the organization along the axis is affected by the interaction of the 'wings' of the bowties, whose position depends on ϕ. Because d is mostly insensitive to ϕ, the helix pitch, which is proportional to d/Ω, scales like ϕ^{-1} for small ϕ.

---

[1] L. Paramonov and S. N. Yaliraki, J. Chem. Phys. **123**, 194111 (2005).

[2] J. W. Perram and M. Wertheim, J. Comp. Phys. **58**, 409 (1985).

[3] J. W. Perram, J. Rasmussen, E. Præstgaard, and J. L. Lebowitz, Phys. Rev. E **54**, 6565 (1996).

[4] S. N. Fejer and D. J. Wales, Phys. Rev. Lett. **99**, 086106 (2007).

[5] M. R. Hoare and J. McInnes, Faraday Discuss. Chem. Soc. **61**, 12 (1976).

[6] J. P. K. Doye, M. A. Miller, and D. J. Wales, J. Chem. Phys. **110**, 6896 (1999).

[7] J. P. K. Doye and D. J. Wales, J. Chem. Phys. **116**, 3777 (2002).

[8] R. Thom, *Stabilité Structurelle et Morphogénèse* (Benjamin, 1972).

[9] D. J. Wales, Science **293**, 2067 (2001).